

Landau theory of charge and spin ordering in the nickelates

SungBin Lee,¹ Ru Chen,¹ and Leon Balents²

¹*Physics Department, University of California, Santa Barbara, CA, 93106*

²*Kavli Institute for Theoretical Physics, University of California, Santa Barbara, CA, 93106-9530*

(Dated: October 25, 2018)

Guided by experiment and band structure, we introduce and study a phenomenological Landau theory for the unusual charge and spin ordering associated with the Mott transition in the perovskite nickelates, with chemical formula RNiO_3 , where $\text{R}=\text{Pr, Nd, Sm, Eu, Ho, Y, and Lu}$. While the Landau theory has general applicability, we show that for the most conducting materials, $\text{R}=\text{Pr, Nd}$, both types of order can be understood in terms of a nearly-nested spin density wave. Furthermore, we argue that in this regime, the charge ordering is reliant upon the orthorhombic symmetry of the sample, and therefore proportional to the magnitude of the orthorhombic distortion. The first order nature of the phase transitions is also explained. We briefly show by example how the theory is readily adapted to modified geometries such as nickelate films.

The nature of the Mott metal-insulator transition (MIT), driven by Coulomb repulsion between electrons, is a central subject in condensed matter physics. A canonical MIT occurs in the nickelates, perovskites with the composition RNiO_3 , where R is a rare earth with nominal valence R^{3+} . Metallicity in the nickelates correlates with ionic radius, varying from largest, $\text{R}=\text{La}$, which is metallic at all temperatures, to smallest, $\text{R}=\text{Lu}$, which is insulating at all temperatures; $\text{R}=\text{Eu}$ has the highest MIT temperature, $T_{\text{MIT}} = 480\text{K}$.¹ The nickelates are particularly interesting because they display complex ordering phenomena in the insulating state. The insulating ground states are magnetic, with a large unit cell corresponding to a periodicity of 4 lattice spacings relative to the ideal cubic structure, and is usually interpreted in terms of an “up-up-down-down” spin configuration. Remarkably, this complex ordering seems to be consistent across the entire family.²⁻⁵ This magnetism coexists with a form of “Charge Ordering” (CO), which modulates the Ni charge from $\text{Ni}^{3+\delta}$ to $\text{Ni}^{3-\delta}$ on alternating sites of a rock-salt type substructure of the cubic perovskite. In the more insulating nickelates, $\text{R}=\text{Eu, Ho}$, this charge ordering occurs not only in the ground state but also in an intermediate temperature insulating phase without magnetism between the high-temperature metallic phase and the low temperature magnetic one.

It has been postulated that the charge ordering is fundamental, and should be thought of as separation into spinless Ni^{4+} and spin $s = 1$ Ni^{2+} ions, due to dominant local Hund’s rule coupling J_H .⁶ However, no explanation has been given for the particular complex yet robust magnetic structure in this picture. Moreover, in the materials PrNiO_3 and NdNiO_3 , for which the MIT occurs at relative low temperature, the ionic description does not seem so natural. In addition, in these materials, charge and spin order occur simultaneously, bringing the primacy of the former into question.

In this paper, we introduce a phenomenological Landau theory, motivated by the particular structure of the e_g bands of the nickelates near the Fermi energy. It is particularly relevant to the more itinerant materials such as PrNiO_3 and NdNiO_3 , where charge and spin ordering

are coincident, and the Landau theory has a natural microscopic origin in a spin density wave (SDW) picture. The SDW picture and Landau theory yield a number of direct insights into the ordering in bulk samples. First, the observed unusual magnetic periodicity is simply explained due to approximate *Fermi surface nesting* of the e_g bands. Second, we argue that the observed charge ordering is naturally induced in this picture as a *secondary order parameter*. Third, the magnitude of the induced charge order is *proportional to the degree of orthorhombicity* in the material, a correlation which is indeed observed in experiments, though the causative relationship does not appear to have been identified previously.

The Landau theory can also be easily adapted to other situations. As one such application, we derive the a general phase diagram describing the passage from “weak” (SDW-like) Mott insulators to “strong” Mott insulators, in which charge ordering is indeed dominant, which is in agreement with that observed in the bulk nickelates, and we explain the first order nature of the transitions observed there. We also show how to incorporate the effects of strain and interfaces in films and multilayers, and predict that changes of the magnetic ordering wavevector and exotic “multiple- q ” states may be thus induced.

Microscopic considerations: It is helpful to consider as a semi-microscopic model framework a tight-binding description of the e_g bands,

$$H_{tb} = - \sum_{ij} t_{ij}^{ab} c_{ia\sigma}^\dagger c_{j b\sigma}, \quad (1)$$

where i, j are site indices, $a, b = 1, 2$ are orbital indices denoting the two e_g states with the symmetry of $2z^2 - x^2 - y^2$ and $x^2 - y^2$ orbitals (these should properly be considered hybridized combinations – Wannier functions – of Ni d states and the neighboring O p states, as RNiO_3 is a charge transfer insulator), and $\sigma = \uparrow, \downarrow$ is the spin index. Sums over orbital and spin indices are implied. The dominant hopping processes are expected to be those with σ -type bonding, which can occur with amplitude t and t' when i, j are first and second neighbor sites, respectively, of the ideal cubic Ni sublattice. Specifically,

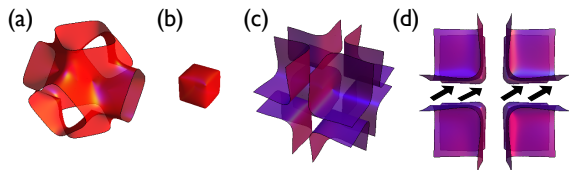


FIG. 1: Fermi surfaces for the tight-binding model. In (a) and (b), we show the conduction and valence band Fermi surfaces, respectively, for $t'/t = 0.1$. For larger t'/t , the conduction band Fermi surfaces become large and hole-like, as shown in (c) and (d) for $t'/t = 0.3$. The approximate nesting in the latter case is indicated schematically in (d).

then $t_{i,i\pm\hat{\mu}}^{ab} = t\phi_{\mu}^a\phi_{\mu}^b$ and $t_{i,i\pm\hat{\mu}\pm\hat{\nu}}^{ab} = t'(\phi_{\mu}^a\phi_{\nu}^b + \phi_{\mu}^b\phi_{\nu}^a)$, where $\phi_x = (-\frac{1}{2}, \frac{\sqrt{3}}{2})$, $\phi_y = (-\frac{1}{2}, -\frac{\sqrt{3}}{2})$, $\phi_z = (1, 0)$ are the orbital wavefunctions for the $2x^2 - y^2 - z^2$, $2y^2 - x^2 - z^2$, and $2z^2 - x^2 - y^2$ σ -bonding orbitals along the three axes, in the chosen basis, respectively.

The above tight-binding model agrees with the e_g bands obtained from LDA calculations,⁷ and the Fermi surface measured recently in photoemission on a LaNiO_3 film.⁸ It also explains well resistivity, Hall effect, and thermopower measurements on LaNiO_3 films,⁹ and approximately describes the inter-band optical spectral weight at energies below about 1eV.¹⁰ LDA favors $t'/t \approx 0.1$, while comparison to photoemission is best for $t'/t \approx 0.3$, and the range $0.1 \leq t'/t \leq 0.4$ is consistent with transport. It is instructive to view the Fermi surface for this range of values (see Fig.1). One observes in the middle of this range that the Fermi surface is rather flat and approximately composed of “cubes” rather than spheres. Fermi surfaces with large flat sections are considered approximately “nested”, and well-known to lead to enhance susceptibilities at certain wavevectors. Calculation of the free electron spin susceptibility (see Fig. 2) indeed shows an enhancement, peaked about wavevectors $\langle kkk \rangle$, with k close to $\frac{1}{4}(\times 2\pi)$ (for $t'/t = 0.3$ we find e.g. $k \approx 0.4\pi$). With interactions included, the random phase approximation, or Hartree-Fock theory, both thereby show a tendency to spin-density-wave (SDW) order at wavevectors close to this one. It is remarkable that band theory considerations give a simple mechanism for SDW order at $k = \pi/2$, which corresponds precisely to that observed in *all* the insulating nickelates. Interestingly, we have also found a mechanism for this order in the strong-coupling limit of the appropriate multi-orbital Hubbard model, which is too involved to report here.¹¹ Together, this may explain the robustness of the magnetic state observed in experiment. This unusual magnetic order has not, to our knowledge, been explained before by any theory.

Landau theory: Rather than proceeding with a microscopic theory (Hartree-Fock and other calculations will be reported in a future publication¹¹), we instead pursue the implications of this view using symmetry-based Landau analysis. We begin by considering the problem for an ideal cubic solid, and take into account distortions of

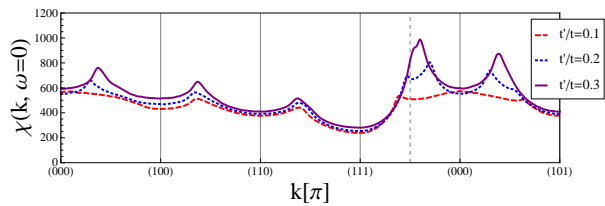


FIG. 2: Zero frequency spin susceptibility for the tight-binding Hamiltonian for $t'/t = 0.1, 0.2, 0.3$, as a function of momentum \mathbf{k} in the cubic Brillouin zone. Note that for the best nested situation, $t'/t = 0.3$, the susceptibility is sharply peaked close to the wavevector $2\pi(\frac{1}{4}, \frac{1}{4}, \frac{1}{4})$.

the perovskite structure at a later stage. For the SDW order, states with wavevectors along *any* of the $\langle 111 \rangle$ axes are equivalent. Hence we actually need to include *four* order parameters, ψ_a with wavevectors \mathbf{Q}_a , given by $\mathbf{Q}_0 = \frac{\pi}{2}(1, 1, 1)$, $\mathbf{Q}_1 = \frac{\pi}{2}(1, -1, -1)$, $\mathbf{Q}_2 = \frac{\pi}{2}(-1, 1, -1)$, and $\mathbf{Q}_3 = \frac{\pi}{2}(-1, -1, 1)$. Physically, the meaning of the order parameters, which are complex vectors, is that

$$\langle \mathbf{S}_i \rangle = \sum_a \text{Re} [\psi_a e^{i\mathbf{Q}_a \cdot \mathbf{r}_i}]. \quad (2)$$

It is a straightforward but lengthy exercise to identify all the allowed terms, up to fourth order in the SDW order parameters, in the Landau expansion, taking into account the translational and point group symmetries of the ideal cubic structure. At quadratic order, one obtains only the single coefficient

$$F_2 = r \sum_a \psi_a^* \cdot \psi_a \equiv r \sum_a |\psi_a|^2. \quad (3)$$

At quartic order, one finds 13 distinct terms. We divide them into the three terms involving products of only one “flavor”,

$$F_4^{(1)} = u_1 \sum_a (\psi_a^* \cdot \psi_a)^2 + u_2 \sum_a |\psi_a \cdot \psi_a|^2 + u_3 \left(\sum_a (\psi_a \cdot \psi_a)^2 + \text{h.c.} \right), \quad (4)$$

and ten additional terms involving products of two and four distinct fields. For brevity, we will not give these explicitly here, as they will not play a major role in what follows.

Single-q states: The full free energy simplifies greatly if we restrict to “single-q” states, consistent with experiment. Here only one of the four order parameters is non-zero, and the ten quartic Landau invariants *not* shown in Eq. (4) vanish. In a single-q state, we denote below the non-zero order parameter by simply ψ , without a subscript.

Several types of single-q states are possible, dependent upon values of u_2 and u_3 in $F_4^{(1)}$ in Eq. (4). The second coefficient, u_2 , distinguishes between collinear and spiral states. For $u_2 > 2|u_3|$, minimum energy states have $\psi =$

$\psi(\hat{\mathbf{n}}_1 + i\hat{\mathbf{n}}_2)$, where $\hat{\mathbf{n}}_1$ and $\hat{\mathbf{n}}_2$ are orthogonal unit vectors. These describe coplanar spirals, with spins of fixed length in the plane spanned by $\hat{\mathbf{n}}_1$ and $\hat{\mathbf{n}}_2$. The phase of ψ is arbitrary, corresponding to rotations of the spins within this plane.

For $u_2 < 2|u_3|$, the free energy is minimized by $\psi = \psi\hat{\mathbf{n}}$, where ψ is a complex scalar. Such configurations describe, via Eq. (2), collinear SDW states. In this case, the remaining coefficient, u_3 , selects preferential phases of ψ . Writing $\psi = |\psi|e^{i\theta}$, we finally have

$$F_4^{(1)} = (u_1 + u_2)|\psi|^4 + 2u_3|\psi|^4 \cos 4\theta. \quad (5)$$

When $u_3 < 0$, states with $\theta = \frac{\pi}{2}n$ are favored, while for $u_3 > 0$, states with $\theta = \frac{\pi}{2}(n + \frac{1}{2})$ are favored (in both cases $n = 0, 1, 2, 3$ describe four spatially translated states). Going back to Eq. (2), and using the wavevector $\mathbf{Q}_0 = \frac{\pi}{2}(1, 1, 1)$ and taking $\hat{\mathbf{n}} = \hat{\mathbf{z}}$ for concreteness, we find that these describe spin states with

$$\langle S_i^z \rangle = \begin{cases} |\psi| \times (+1, 0, -1, 0, \dots) & \text{for } u_3 < 0 \\ +\frac{1}{\sqrt{2}}|\psi| \times (+1, -1, -1, +1, \dots) & \text{for } u_3 > 0 \end{cases}, \quad (6)$$

where the successive terms in parenthesis describe successive spin expectation values when moving in unit steps along the principle cubic x, y , or z axes in real space.

Charge order: For the three types of magnetic states found above (one spiral, two collinear), let us consider the associated charge order. We consider charge ordering at the wavevector (π, π, π) , corresponding to the ‘‘rock salt’’ ordering observed in experiment. The order parameter Φ is introduced via

$$\langle n_i \rangle = \bar{n} + (-1)^{x_i+y_i+z_i}\Phi, \quad (7)$$

where $n_i = \sum_{a\sigma} c_{ia\sigma}^\dagger c_{ia\sigma}$ is the electron number operator. Φ may equally well be regarded as representing the amplitude of optical phonons representing octahedral breathing modes at the same wavevector. Symmetry allows the following terms in the free energy involving Φ

$$F_\Phi = \tilde{r}\Phi^2 + \tilde{u}\Phi^4 - \lambda\Phi \sum_a \text{Re}[\psi_a \cdot \psi_a], \quad (8)$$

where we have included the leading linear coupling to the SDW order parameters. The crucial thing to note here is that whenever $\psi \cdot \psi$ is real and non-zero, a non-zero Φ is necessarily induced in the minimum free energy state. In such situations, Φ is a *secondary order parameter*, slaved to the primary SDW one. Mathematically, if \tilde{u} can be neglected, Φ can be readily ‘‘integrated out’’ (F_Φ can be minimized with respect to Φ) to simply renormalize the quartic SDW couplings.

In this case, we can analyze charge order simply in terms of the SDW states. In two of the three SDW states discussed above, the spiral and the collinear state with $\theta = \pi/4$, $\text{Re}[\psi \cdot \psi] = 0$, the charge order vanishes. This is easily understood since in these cases all sites have equivalent spin states, up to rotations. In the remaining collinear state, with $\theta = 0$, $\text{Re}[\psi \cdot \psi] = |\psi|^2$ and

$\Phi \neq 0$. Again this is intuitively clear since the sites with zero spin are obviously distinct from those with non-zero spin. Two problems arise now in comparison with experiment. First, we must arbitrarily choose parameters to be in the third magnetic state in order to obtain the observed charge order. Second, in experiment, non-zero magnetic moments, of unequal magnitude, are clearly observed on the two types of ‘‘inequivalent’’ sites, while in this theoretical configuration the magnetic moment vanishes on half the sites.

Orthorhombicity: These problems are resolved by taking into account the distortions of the ideal perovskite structure. We focus on the orthorhombic (Pbnm) structure, which obtains for all the nickelates except LaNiO_3 , which is rhombohedral, and does not undergo a Mott transition. The orthorhombic distortion is present in the metallic state up to high temperatures (e.g. up to $T = 780\text{K}$ in PrNiO_3 ¹²), and is understood to arise from reduction in the tolerance factor due to the changing rare earth ionic radius. The Pbnm space group has only discrete reflection and inversion operations in its point group. The structure has a quadrupled unit cell, which is doubled by a 45° rotated, approximately $\sqrt{2} \times \sqrt{2}$ enlarged supercell in the $a-b$ plane, and a doubling along the c axis. One can rewrite the conventional cubic coordinates x, y, z in terms of standard orthorhombic coordinates x, y, z , according to $x = x + y - \frac{1}{2}$, $y = -x + y + \frac{1}{2}$, $z = 2z$. Making this transformation, one finds that the 4 cubic SDW states corresponds to two orthorhombic SDW wavevectors: $Q_0^{\text{ortho}} = Q_3^{\text{ortho}} = 2\pi(0, \frac{1}{2}, \frac{1}{2})$ and $Q_1^{\text{ortho}} = Q_2^{\text{ortho}} = 2\pi(\frac{1}{2}, 0, \frac{1}{2})$. The latter is the wavevector found in experiments on nickelates with $R=\text{Sm, Eu, Nd, Pr, and Ho}$.²⁻⁵

The Pbnm space group has considerably lower symmetry than cubic, containing only inversion, reflection, and 180° screw axes apart from translations. As a consequence, the orthorhombic distortion allows additional terms in the Landau free energy. A straightforward analysis shows that two such terms arise at quadratic order:

$$F_2^{\text{ortho}} = r_1(|\psi_0|^2 - |\psi_1|^2 - |\psi_2|^2 + |\psi_3|^2) + r_2(\psi_1 \cdot \psi_1 - \psi_2 \cdot \psi_2 + \text{c.c.}). \quad (9)$$

We neglect orthorhombic corrections to the quartic terms on the grounds that they are presumably smaller.

The terms in Eq. (9) clearly lead to an energy difference between the two possible orthorhombic wavevectors. We focus on the case $r_1 > -|r_2|$, for which ordering in ψ_1, ψ_2 is preferred, which corresponds to the experimental wavevector. To proceed, we suppose, without loss of generality, that $\psi_1 = \psi$ is the non-zero order parameter. For the spiral state, we now consider the cubic energy from Eq. (4), with $u_2 > 0$, added to the r_2 term. For r_2 non-zero, the minimum energy configuration is deformed to $\psi \propto (1 + \delta)\hat{\mathbf{n}}_1 + i(1 - \delta)\hat{\mathbf{n}}_2$, with $\delta \propto r_2$. This corresponds to a deformed spiral in which spins trace out an ellipse rather than a circle. In this state, $\Phi \propto \psi \cdot \psi \propto r_2$, so charge order is induced.

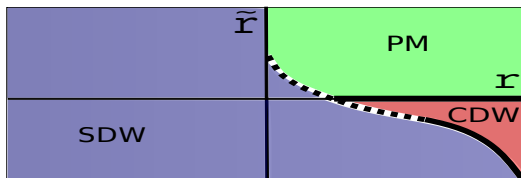


FIG. 3: Mean-field phase diagram for the Landau theory of Eq. (11), describing the interplay of spin and charge ordering. The dashed (solid) lines delineate first (second) order transitions within mean field theory.

For the collinear state, Eq. (5) is modified to

$$F(\theta) = F_0 + 2u_3|\psi|^4 \cos 4\theta + 2r_2|\psi|^2 \cos 2\theta. \quad (10)$$

There are two cases to consider here. For $u_3 < 0$, both cosines can be simultaneously minimized. The minimum in this case occurs at either $\theta = \frac{\pi}{2}n$, with integer n either even or odd if r_2 is negative or positive, respectively. This selects the $+1, 0, -1, 0, \dots$ type ordering in the first line of Eq. (6).

In the other case, $u_3 > 0$, the situation is more interesting. The minimum at $\theta = \frac{\pi}{2}(n + 1/2)$ are *unstable* to small r_2 of either sign. Thus the generic situation in this case, at least for small $|r_2|$, is to obtain a generic value of $0 < \theta < \pi/4$. (For sufficiently large r_2 , the minimum θ will again lock to the above type of solution). As a result, one obtains the type of order observed in experiment.

The conclusion is that in the $Q_{1/2}^{\text{ortho}} = 2\pi(\frac{1}{2}, 0, \frac{1}{2})$ state, the SDW is *always* accompanied by charge order due to orthorhombicity. Moreover, if the state is such that moments are present on all sites, then the charge order is *proportional* to the degree of orthorhombicity, parametrized here by r_2 . This is an important conclusion of this paper. Interestingly, if the analysis is repeated for a *rhombohedral* ($R\bar{3}c$) crystal, no charge order is induced in this way.¹¹ Hence for a rhombohedral insulator,¹³ we predict the occurrence of a “pure” SDW state.

Order of transitions: The three phase transitions – metal-CO, metal-SDW, and CO-SDW – observed in experiment are all first order. This behavior can be rationalized by various mechanisms. First consider a mean-field treatment of the Landau free energy. For simplicity, we assume single-q states, and neglect the distinctions

between collinear and spiral spin states, taking $\psi = \psi\hat{x}$ with ψ real. Then the full Landau free energy is

$$F = r\psi^2 + u\psi^4 - \lambda\Phi\psi^2 + \tilde{r}\Phi^2 + \tilde{u}\Phi^4. \quad (11)$$

By minimizing this free energy, one obtains the phase diagram shown in Fig. 3. For $\lambda = 0$, the SDW and CO orders are tuned independently by r and \tilde{r} respectively. However, with non-zero spin-charge coupling λ , the region near the origin is modified. In particular, the consequence is that for systems close to the multicritical point at which the CO phase emerges, all the transitions to the SDW phase become first order. This may explain the discontinuous SDW transitions seen in experiment. To explain the first order metal-CO transition, we note that electron-phonon interactions are significant in nickelates.¹⁴ In particular coupling of Φ to *acoustic phonons* renders the theory of the metal-CO transition equivalent to the *compressible Ising model*, which is known to have a first order transition.¹⁵

Films: We conclude with examples of how the Landau theory is adapted to modified geometries. Pure strain is relevant to thick films in which interfaces are not important. For a tetragonal substrate, symmetry implies that the strain modifies r (Eq. (3)) and r_1 (Eq. (9)). If the intrinsic orthorhombic contribution to r_1 is small, we predict that strain can switch the wavevector from $Q_{1/2}^{\text{ortho}}$ to $Q_{0/3}^{\text{ortho}}$, and at the same time “turn off” the charge ordering. A more severe effect occurs at an interface, due to the lack of translational symmetry normal it. This leads to symmetry-allowed terms which *mix* the SDW states with wavevectors Q_1 and Q_2 (or Q_0 and Q_3), so that “multiple-q” ordering appears near the interface.

Acknowledgments

We are grateful to Susanne Stemmer, Jim Allen, Dan Ouellette, and Junwoo Son for discussions and experimental inspiration. This work was supported by the NSF through grants PHY05-51164 and DMR-0804564, and the Army Research Office through MURI grant No. W911-NF-09-1-0398.

¹ J. Torrance et al., Phys. Rev. B **45**, 8209 (1992).

² M. T. Fernández-Díaz et al., Phys. Rev. B **64**, 144417 (2001).

³ J. Rodríguez-Carvajal et al., Phys. Rev. B **57**, 456 (1998).

⁴ J. L. García-Muñoz et al., Phys. Rev. B **50**, 978 (1994).

⁵ J. García-Muñoz et al., Europhys. Lett **20**, 241 (1992).

⁶ I. Mazin et al., Phys. Rev. Lett **98**, 176406 (2007).

⁷ N. Hamada, J. Phys. Chem. Solids **54**, 1157 (1993).

⁸ R. Eguchi et al., Phys. Rev. B **79**, 115122 (2009).

⁹ J. Son et al., Appl. Phys. Lett **96**, 062114 (pages 3) (2010).

¹⁰ D. G. Ouellette et al., Phys. Rev. B (2010), submitted.

¹¹ S. B. Lee et al., in preparation.

¹² P. Lacorre et al., J. Solid. State. Chem **91**, 225 (1991).

¹³ J. Vassiliou et al., J. Solid. State. Chem **81**, 208 (1989).

¹⁴ M. Medarde et al., Phys. Rev. Lett. **80**, 2397 (1998).

¹⁵ D. J. Bergman et al., Phys. Rev. B **13**, 2145 (1976).